CDF/DOC/BOTTOM/CDFR/4980
Version 0
May 13, 1999

Some Initial Tests of the Photomultiplier Tubes for the CDF Time-of-Flight Detector

A. Kazama, T. Asakawa, F. Ukegawa and S. Kim
University of Tsukuba

Abstract

Two Hamamatsu R5946mod fine-mesh photomultiplier tubes have been tested for their timing performance using precision laser light and cosmic rays. We find that intrinsic timing resolution of the photomultiplier tubes is much better than 100 ps, an overall goal of the CDF time-of-flight detector.

1 Introduction

The CDF time-of-flight (TOF) system resides in the solenoid and the photomultiplier tubes (PMTs) have to work in the presence of the 1.4 T axial magnetic field. The current choice of the PMT is Hamamatsu R5946mod, a 19-stage version of the original R5946 tube (16 stages). They both use fine-mesh dynodes for operation in a magnetic field.

The 19-stage version has been developed in the past couple of years by request from CDF. Several tubes have been produced recently and a few have been delivered to Penn (2 tubes) and to Tsukuba (5 tubes). The PMT is 38 mm (1.5 inches) in diameter and 50 mm long, with long semi-flexible leads. The minimum diameter of the sensitive area is 27 mm. The tubes are operated with a positive high voltage with grounded cathode. Two of the tubes delivered to Tsukuba, with serial numbers ZH5122 and ZH5126, have been equipped with a base assembly made by Hamamatsu. All other tubes have no bases, and bases (and preamplifiers) made at Penn will be installed.

Hamamatsu provided us with data sheets that show the results of several measurements done at Hamamatsu. We reproduced one of them in Table 1, which shows cathode and anode luminous sensitivity measured in DC mode using a tungsten lamp as a light source. A typical current amplification ("gain") of 7×10^7 is observed at a high voltage of 2000 V. This particular list includes tubes other than those CDF has purchased. Other test data for selected tubes include measurements of gains, and the transit time spread (TTS) for single

R5946MOD (19 stages) DC Sensitivity

Serial Number		Cathode luminous sensitivity (μA/lm)	Anode luminous sensitivity (A/lm)	Anode dark current (nA)	Cathode blue sensitivity (μA/lm-blue)	Gain (10^6)
ZH5121	(Penn)	77.0	7260	150	9.71	94.3
ZH5122*	(Tsukuba)	51.9	8050	16.00	8.4	155.1
ZH5123	(Penn)	76.5	4610	7.20	9.83	60.3
ZH5125		74.6	2710	77	10.0	36.3
ZH5126*	(Tsukuba)	81.5	5320	9.30	10.1	65.3
ZH5127		72.6	6820	34	9.8	93.9
ZH5128		57.4	4380	2.4	9.0	76.3
ZH5129	(Tsu $\rightarrow$ P)	75.4	11400	11.00	9.9	151.2
ZH5130		79.5	7230	9.4	10.0	90.9
ZH5131		65.2	3230	2.2	9.2	49.5
ZH5132	(Tsu $\rightarrow$ P)	82.7	2080	1.10	10.4	25.2
ZH5133		64.0	2200	9.6	9.4	34.4
ZH5134		58.3	1730	1.0	9.2	29.7
ZH5135		63.4	7540	7.4	9.9	118.9
ZH5136	(Tsukuba)	76.5	3680	2.50	10.2	48.1
ZH5137		87.9	2040	1.7	10.4	23.2
						Typ 71.3

Table 1: Cathode and anode luminous sensitivity of R5946mod tubes. Reproduced from data sheet provided by Hamamatsu. Measurements of anode sensitivity and dark current are made at a high voltage of 2000 V. Tubes with (*) are equipped with base assembly made by Hamamatsu.

photoelectrons, both with and without magnetic fields. A plot shows the relative gains of six tubes as a function of an axial magnetic field up to 1.5 T. At 1.5 T, the tubes show a reduction in the gain by a factor of about 1000. If we assume that secondary electrons are lost evenly in 19 dynode stages, it means that each stage sufffers a loss of gain by a factor of 0.695 ($0.695^{19} = 1/1000$). Another interesting measurement by Hamamatsu is the TTS for single photoelectrons. It is measured for tubes ZH5122 and ZH5126. The FWHM values at 0 T are 376 ps and 412 ps for the two tubes, respectively, and at 1.5 T they are 577 ps and 429 ps. These data sheets have been scanned and are available on the web pages:

```
http://hep-www.px.tsukuba.ac.jp/~ukegawa/tof/9903/
http://hep-www.px.tsukuba.ac.jp/~ukegawa/tof/990415/
```

Since R5946mod tubes have never been used or tested anywhere outside Hamamatsu, we have made some initial measurements of their characteristics, timing resolution in particular. We have used a precision diode laser system that can emit blue light with small time jitter, injected light to the PMTs and measured the timing resolution. We have also used cosmic rays and scintillation light in order to mimic the conditions created by real collision particles.

We have tested the two tubes with the Hamamatsu base, and find the results satisfactory. Although the tests are done without any substantial magnetic field, past tests show that the PMT performance does not degrade much when used in a 1.4 T field. We are therefore reasonably confident that the PMTs, at least the ones we have tested, are adequate for the CDF TOF detector.

2 Tests using precision laser light

We have made some measurements using laser light. We first describe the laser system. It is Hamamatsu PLP-02, and consists of a precision pulser and a laser diode head. The time jitter of emitted light with respect to the trigger pulse from the pulser is claimed to be less than 10 ps. Since we are trying to measure resolutions of about 50 to 100 ps, this jitter should be more than adequate. The laser head contains a diode laser and a frequency doubler crystal so that photons of 415 nm wavelength will be emitted. This almost matches the peak emission wavelength of 425 nm from Bicron BC408 scintillator.

Because it is a diode laser it does not require gases and so it is very easy to operate. The precise timing, output stability, and the wavelength matched to scintillation light and the PMT sensitivity make it a very useful and attractive device for the present test purposes. We have tried to purchase one, but unfortunately Hamamatsu has discontinued the model with a laser head that can emit light of the short wavelength (415 nm). Fortunately one of our colleagues in the Nuclear Physics Group of the University has this laser system and kindly let us use it for the tests described here.

Tube	HV	thr. = 50 mV		thr. = 30 mV	
		σ_{TDC}	σ_t	σ_{TDC}	σ_t
	(V)	(count)	(ps)	(count)	(ps)
ZH5122	900	17.07	450	7.82	196
	1150	3.00	75	2.80	70
	1200	2.48	62	2.58	65
ZH5126	1150	7.51	188	5.39	135
	1350	3.55	89	3.05	76
	1500	2.50	62	2.63	66

Table 2: Width of TDC arrival time distributions for laser light.

2.1 Timing resolution

The main purpose of the test is to measure the timing resolution of the PMTs. If the resolution is not better than 100 ps, it would not make much sense to hope that the final TOF detector can achieve a 100 ps resolution.

The setup of the measurement is shown in Figure 1. We use a CAEN C414 CAMAC TDC, which can be set to a resolution of 25 ps per count. The trigger signal from the pulser is used to start the TDC. The laser light is directed to the PMT placed in front of the laser head. The analog signal from the PMT is discriminated and the output NIM signal is used to stop the TDC. We have used a conventional discriminator. We have operated the laser with internal clock mode at a frequency of about 10 Hz.

The two tubes we tested have the serial numbers ZH5122 and ZH5126. The TDC arrival time distributions are shown in Figures 2 and 3 for the two tubes. Each figure shows distributions with different high voltage settings. The pulse heights from ZH5122 observed on a scope are roughly 250 mV, 500 mV and 1 V. The discriminator threshold is set to 50 mV. The widths of the time distributions are 450, 75 and 62 ps for ZH5122, and 188, 89 and 62 ps for ZH5126. They are summarized in Table 2. It is obvious that the 50 mV threshold of the discriminator is not adequate when pulses are as small as 250 mV. However, it works well once the pulse height reaches as high as 500 mV, and better for 1 V pulses.

Figures 4 and 5 show the corresponding TDC arrival time distributions when the discriminator threshold is lowered to 30 mV. The results are even better, with resolutions of 196, 70 and 65 ps for ZH5122, and 135, 76 and 66 ps for ZH5126.

One question a reader might have at this point would be how many photons we have been injecting. We have tried to inject light that corresponds to minimum ionizing particles. To check this we had previously looked on a scope at pulses for cosmic rays penetrating 4 cm thick BC408 scintillator. We saw pulses of about 1 V at a high voltage of 1200 V for ZH5122. Therefore, we adjusted the laser output so that we get a similar pulse height from

Tube	HV (V)	$\langle$ADC$\rangle$ (count)	ped. (count)	peak (count)	peak (pC)	σ_{ADC} (count)	σ/peak	$N_{\text{p.e.}}$	Est. gain
ZH5122	900	106.9	72.1	34.8	10.4	2.99 ± 0.05	0.086	≥ 135	4.8×10^5
	1150	353.0	72.2	280	84.0	23.5 ± 0.4	0.084	≥ 142	3.7×10^6
	1200	409.4	72.2	336.6	101.0	29.3 ± 0.6	0.087	≥ 132	4.8×10^6
ZH5126	1150	131.0	72.4	58.6	17.6	4.74 ± 0.08	0.081	≥ 153	7.2×10^5
	1350	283.5	72.5	210.8	63.2	16.8 ± 0.3	0.080	≥ 157	2.5×10^6
	1500	563.6	72.4	490.4	147.1	37.9 ± 0.9	0.077	≥ 167	5.5×10^6

Table 3: Mean and width of ADC pulse height distributions for laser light.

the laser, by inserting a 20% neutral density filter between the laser head and the PMT. As we shall see later, this turns out to be an underestimate for the number of photons for cosmic rays by about a factor of two. Therefore, the timing resolutions quoted above can still be improved.

2.2 Pulse height measurements

We have measured the pulse heights for the laser light using the setup shown in Figure 6. We use a KAIZU 5010 ADC, which has 12 bits with 0.3 pC per count. Pulse height distributions for the two tubes are shown in Figures 7 and 8, where we have also tried the three high voltage settings. The mean and width of the distributions are given in Table 3, along with the relative width calculated from these numbers. The mean pulse height as a function of the applied high voltage is shown in Figure 9.

From the width of the pulse height distributions one can get some ideas about the number of photoelectrons the PMTs are seeing. The number of photoelectrons produced at the photocathode and subsequently detected by the dynodes should follow a Poisson distribution. If the average number is $N_{\text{p.e.}}$, the width of the Poisson distribution should be $\sigma = \sqrt{N_{\text{p.e.}}}$ for a large $N_{\text{p.e.}}$. Thus, we can calculate the number of photoelectrons from the observed width and mean values of the ADC pulse height distributions:

$$N_{\text{p.e.}} = \left(\frac{P_{\text{ADC}}}{\sigma_{\text{ADC}}}\right)^2,$$

where P_{ADC} is the pedestal-subtracted mean pulse height. In reality, there are other factors that contribute to a finite width of pulse height distributions. For example, the pulse height distribution for single photoelectrons is not usually a δ-functuon, and this add to the width of pulse height distributions. Therefore, the number of photoelectrons estimated by this method will always be an underestimate:

$$N_{\text{p.e.}} \geq \left(\frac{P_{\text{ADC}}}{\sigma_{\text{ADC}}}\right)^2.$$

The estimated number of photoelectrons are given in Table 3. We see that the tube ZH5126 gives more photoelectrons than ZH5122. This agrees, at least qualitatively, the Hamamatsu measurements of the cathode luminous sensitivity and cathode blue sensitivity for those tubes (Table 1).

We might expect that the number of photoelectrons increases slowly with an increasing high voltage, because the collection of photoelectrons would be more efficient with a higher voltage between the photocathode and the first stage of the dynodes. Thus, we would expect a shrinkage in the widths with an increasing high voltage value. Figure 10 shows the width of the pulse height distributions as a function of the applied high voltage. This trend seems to be present for ZH5126, but it is not so clear in the case of ZH5122.

From the estimated number of photoelectrons and the charge observed at anode, one can calculate the gain of the PMT. They are listed in Table 3 as well. The gain of the tube ZH5126 is estimated to be 5.5×10^6 at 1500 V. Hamamatsu has provided us with data of the measurements of current amplification measured measured at several high voltage values between 1500 V and 2300 V. Their measurement at 1500 V for ZH5126 shows a current amplification of about 5×10^6 (read from a graph on paper), in good agreement with our estimate above. The Hamamatsu data sheet for current amplification is also available on the web page mentioned earlier.

2.3 Measurements of tube characteristics at several points on the surface of the tube

The measurements described thus far have been made at single points near the middle of the tube. In order to make sure that the points we have made measurements at are not specially good or bad, we have repeated the timing and pulse height measurements at a few points along the surface of the tube ZH5122. We placed the tube on a scanner and moved horizontally with a 5 mm interval (the scanner has a pitch of 1 mm per 2π). Vertically the laser light hits roughly the middle of the tube.

The setup used for this measurement is shown in Figure 11. We split the PMT analog signal using a LeCroy 428F linear fanout, and feed one output to a discriminator for timing measurements and the other to the ADC. However, the timing resolution measured using this split signal showed a degradation from 2.6 counts to 3.5 counts. This means that the fanout has added a time jitter of about 60 ps to the analog signal. This is not quite negligible for the present measurements using laser. Therefore, we have made two measurements at each position: a timing measurement without the fanout (the setup as in Figure 1), and a simultaneous ADC-TDC measurements using the setup including the linear fanout.

The pedestal-subtracted mean pulse height as a function of the position is shown in Figure 12(top). The point at $x = 20$ mm roughly corresponds to the center of the tube, but obviously the eyeball alignment was not quite perfect. The relative positions are rather accurate, though. We observe that the light output is larger than 50% of that at the center in the area as wide as 22 mm.

The bottom plot in the same figure shows the relative width of the pulse height distributions as a function of the position. We see that the width hardly increases at $x = 10$ cm, although the pulse height is only about 50% of that at the center. This result indicates that we do not lose initial photoelectrons much at $x = 10$ cm, but we start to lose secondary electrons at the latter stages of the dynodes (perhaps because of an increase in lateral spread of the secondary electrons) and thus lose the final charge at the anode. The same conclusion can be reached from the data at $x = 35$ mm, where the width roughly doubled but the pulse height decreased about a factor of seven.

The corresponding position dependence of the timing resolution is shown in Figure 13(top). At positions $x = 5$ mm and $x = 37$ mm, the pulse heights are below the discriminator threshold (30 mV) and there are no TDC data.

Figure 13(bottom) shows the mean arrival time as a function of the position. We see that there is a delay of about 4 ns at $x = 35$ mm, which is worrisome if it is a real effect. To check this we investigate the correlation between the arrival time and the pulse height for individual events. This is shown in Figure 14. We see that all events from different positions seem to lie on a single curve that resembles a $1/\sqrt{Q}$ behavior. Therefore, we conclude that the position dependence of the arrival time is only an apparent one.

Although we have made the measurements at a limited number of positions, the observed position dependence of the pulse height and timing resolution seems to reflect the global, mechanical structure of the tube, rather than the variations, e.g. of photocathode sensitivity.

3 Measurements using cosmic rays

In this Section we describe the tests performed using cosmic rays and scintillation light. The setup used for the tests is shown in Figures 15 and 16. We use four layers of 1 cm thick Bicron BC408 scintillator tiles, each having a size of 10 cm by 10 cm by 1 cm. The two R5946mod PMTs are placed to face the 4 cm by 10 cm surfaces of the scintillators through an air gap. We have placed trigger counters on top and bottom of the scintillator, in the middle along the axes of the R5946 PMTs. Each trigger scintillator has a size of 2 cm by 10 cm by 4 mm, and is read out through a light guide with Hamamatsu H1161 PMTs.

The trigger counter signals are discriminated and fed into a coincidence module to provide a start signal for the TDC and a gate for the ADC. The signals from the R5946mod tubes are split with a linear fanout and then fed to the ADC for pulse height measurements and to the TDC through a discriminator. We have set the high voltages to be 1200 V and 1500 V for the tubes ZH5122 and ZH5126. The distriminator threshold is 30 mV for both tubes.

This trigger configuration gives a rate of about 3 events per minute. We took 1000 events. The ADC pulse height and TDC arrival time distributions, as well as their correlation, are shown in Figures 17 and 18 for the tubes ZH5122 and ZH5126, respectively. The minimum ionizing peaks are clearly visible. We notice that the peak pulse heights are about twice as larger as those for laser light at the same high voltage setting (Figures 7 and 8). We had previously tried to adjust the amount of laser light so that it is similar to that from cosmic rays going through the 4 cm thick scintillator. This was done by comparing visually the peak positions of analog signals on a scope. However, we realize that the shapes of the signals are different between cosmic rays and laser (laser light signals are narrower), and this must have resulted in the difference in the amounts of charge observed by the ADC.

The raw TDC time distributions are very wide, with rms widths of 1.6 and 1.8 ns. This is partly because the start time, provided by the trigger counters, has a large jitter. The trigger scintillators are thin, thus not so many photons. Also, the scintillators have a length of 10 cm along the axes of the trigger tubes, and the propagation time of the scintillation light will be different depending on the muon impact position. Those effects will be largely eliminated if we examine the difference in the arrival times measured with ZH5122 and ZH5126. This is shown in Figure 19(top), where we have required the pulse height to be between 500 and 1500 ADC counts for ZH5122, and between 900 and 2500 ADC counts for ZH5126. The width shrinks to 8.4 counts, or 210 ps. Figure 19(bottom) shows the time difference versus the ratio of the pulse heights of the two tubes. A clear correlation is observed, and we correct for it as follows. We examine the time difference distributions in seven slices in the pulse height ratio between 0.4 and 0.75, and approximate the pulse height dependence of the time difference by a linear function of the ratio. We then correct the time difference for each event by subtracting the value of the linear function evaluated at the pulse height ratio observed for that event. The corrected time difference distribution thus obtained is shown in Figure 20, giving a width of 6.0 counts, or 150 ps. This is the resolution for the time difference measured with two tubes, and the resolutions of the individual tubes contribute in quadrature. If we assume that the two tubes have the same resolution, we find 105 ps as a resolution per tube. This is as good as any previous measurements obtained using 16-stage R5946 tubes and cosmic rays.

4 Conclusions

We have tested two of the Hamamatsu R5946mod 19-stage fine-mesh PMTs, to be used for the CDF TOF detector. We find a very good timing resolution (about 65 ps) in both tubes for a modest number of photons from precision laser. The resolution for scintillation light from cosmic rays and scintillator, which should reflect more realistic situations, is not as good, but is still satisfactory.

All the tests described here were done without any magnetic field other than that from the Earth. We should certainly repeat whatever possible tests inside a 1.4 T field. Although we expect that the gain of the tubes will be reduced by a factor of about 1000, we do not expect the timing resolution will be degraded much, as long as we can obtain a reasonable gain by raising the applied high voltage value, because the photoelectron statistics are not expected to be lost much.

Acknowledgment

We would like to thank Professor Yasuo Miake of the Nuclear Physics Group, University of Tsukuba, for letting us use their Hamamatsu pico-second laser.

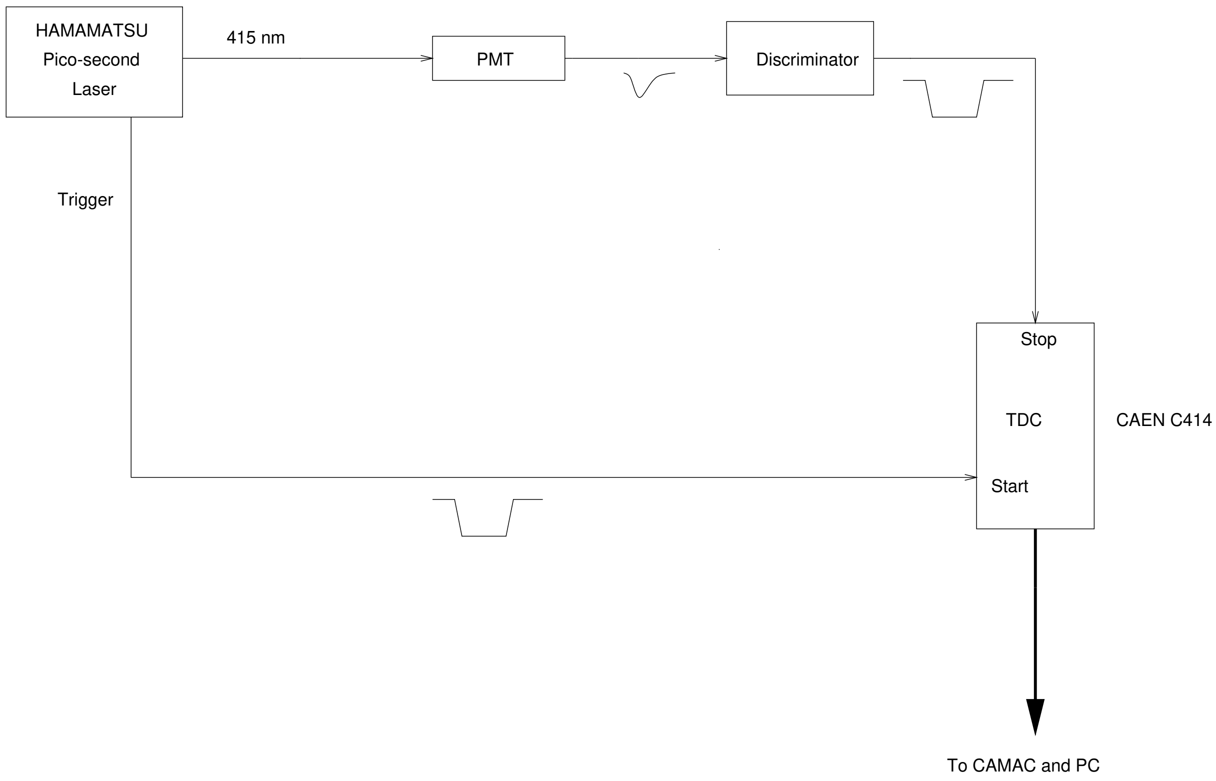

Figure 1: Setup used for the measurement of the PMT timing resolution using a pico-second laser.

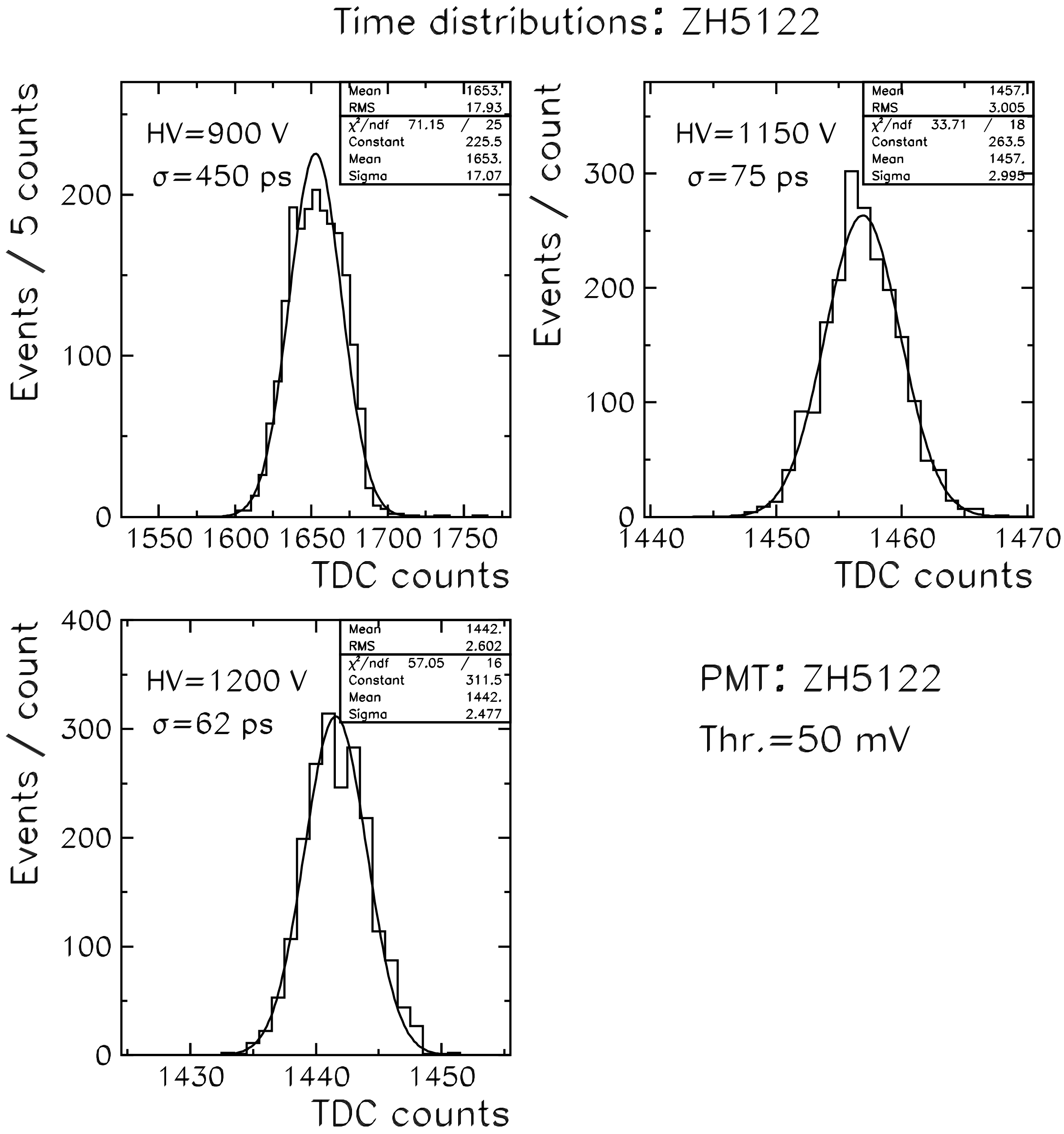

Figure 2: TDC arrival time distributions for pico-second laser light measured with the tube ZH5122. The discriminator threshold is set to 50 mV.

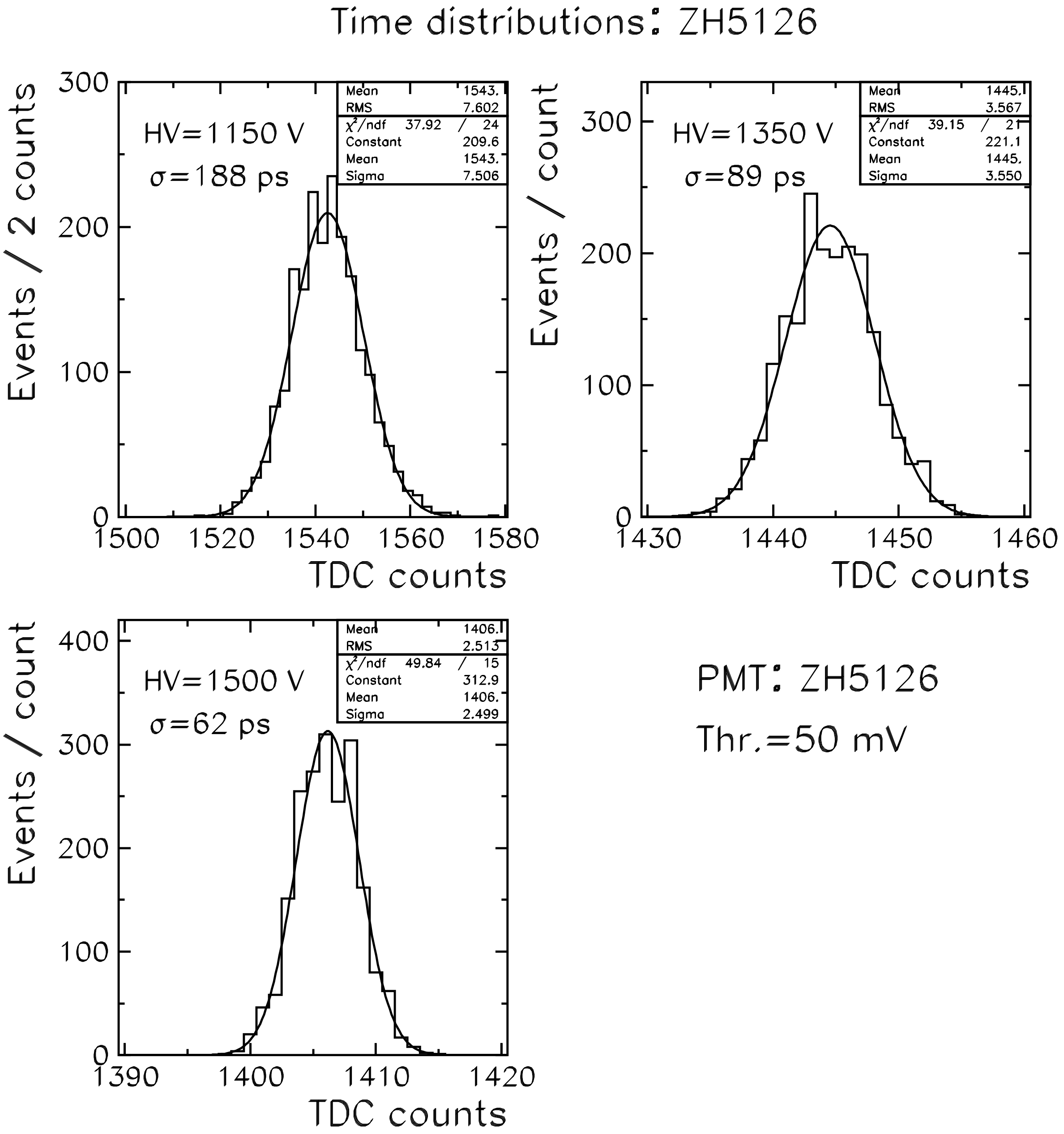

Figure 3: TDC arrival time distributions for pico-second laser light measured with the tube ZH5126. The discriminator threshold is set to 50 mV.

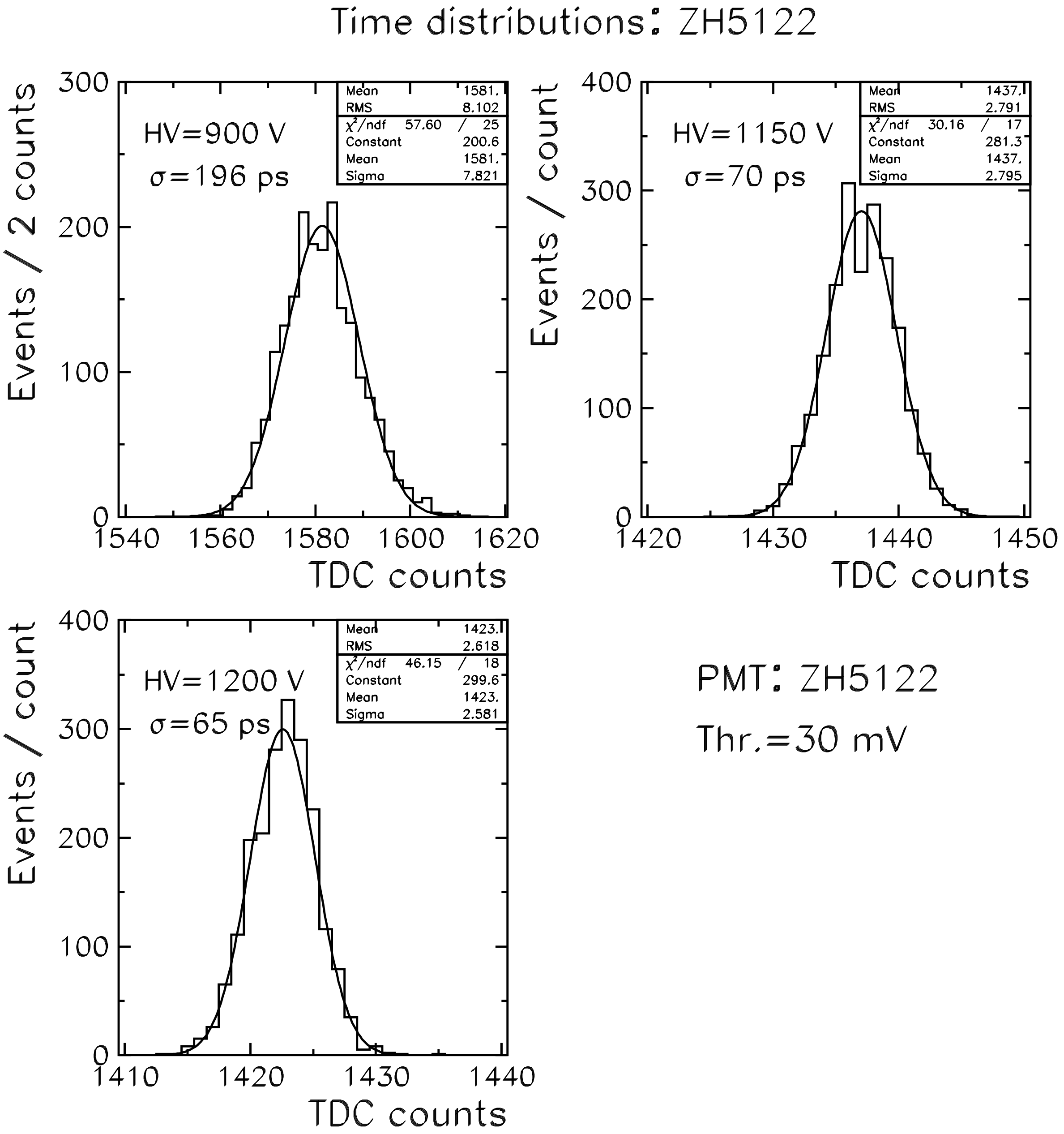

Figure 4: TDC arrival time distributions for pico-second laser light measured with the tube ZH5122. The discriminator threshold is set to 30 mV.

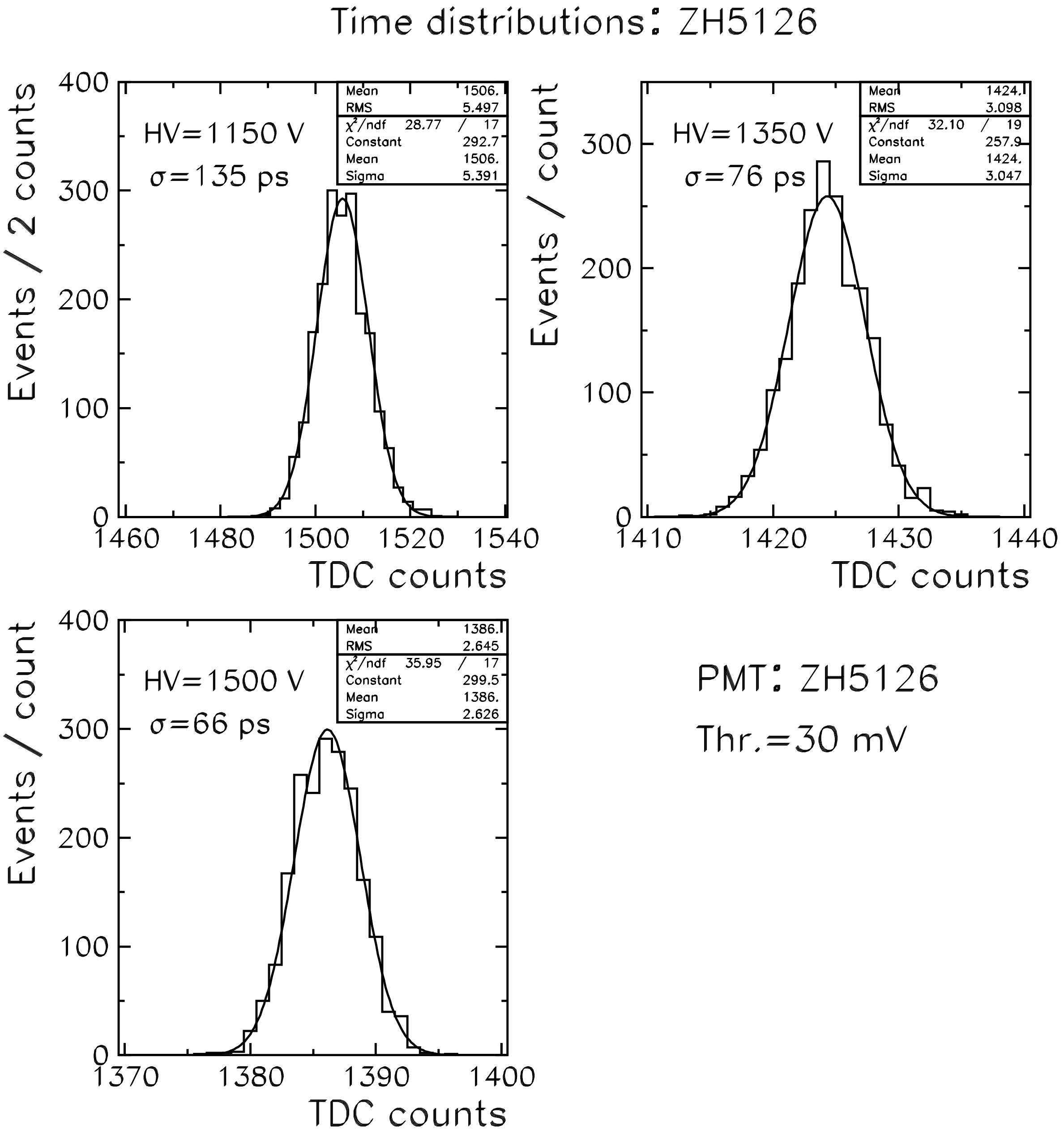

Figure 5: TDC arrrival time distributions for pico-second laser light measured with the tube ZH5126. The discriminator threshold is set to 30 mV.

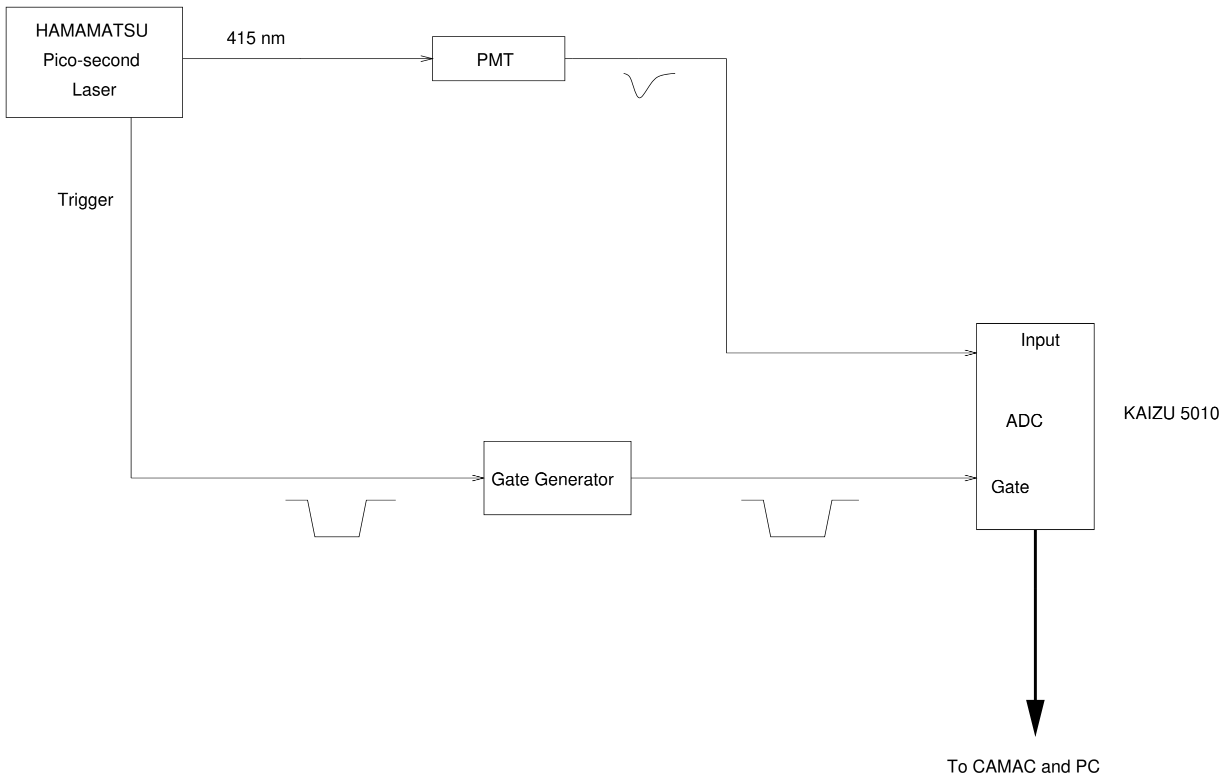

Figure 6: Setup used for the measurement of PMT pulse heights using a pico-second laser.

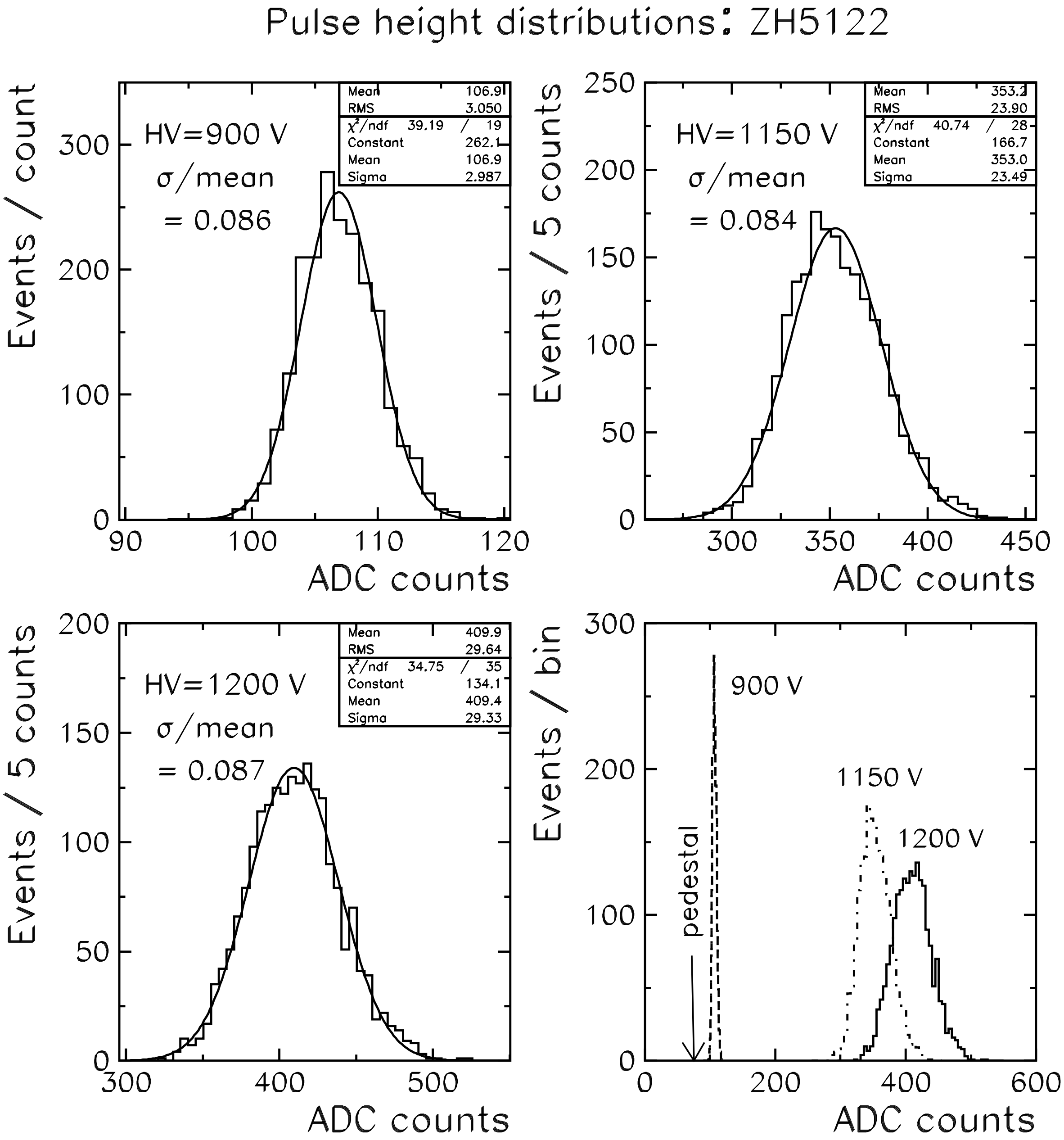

Figure 7: Pulse height distributions for pico-second laser light measured with the tube ZH5122.

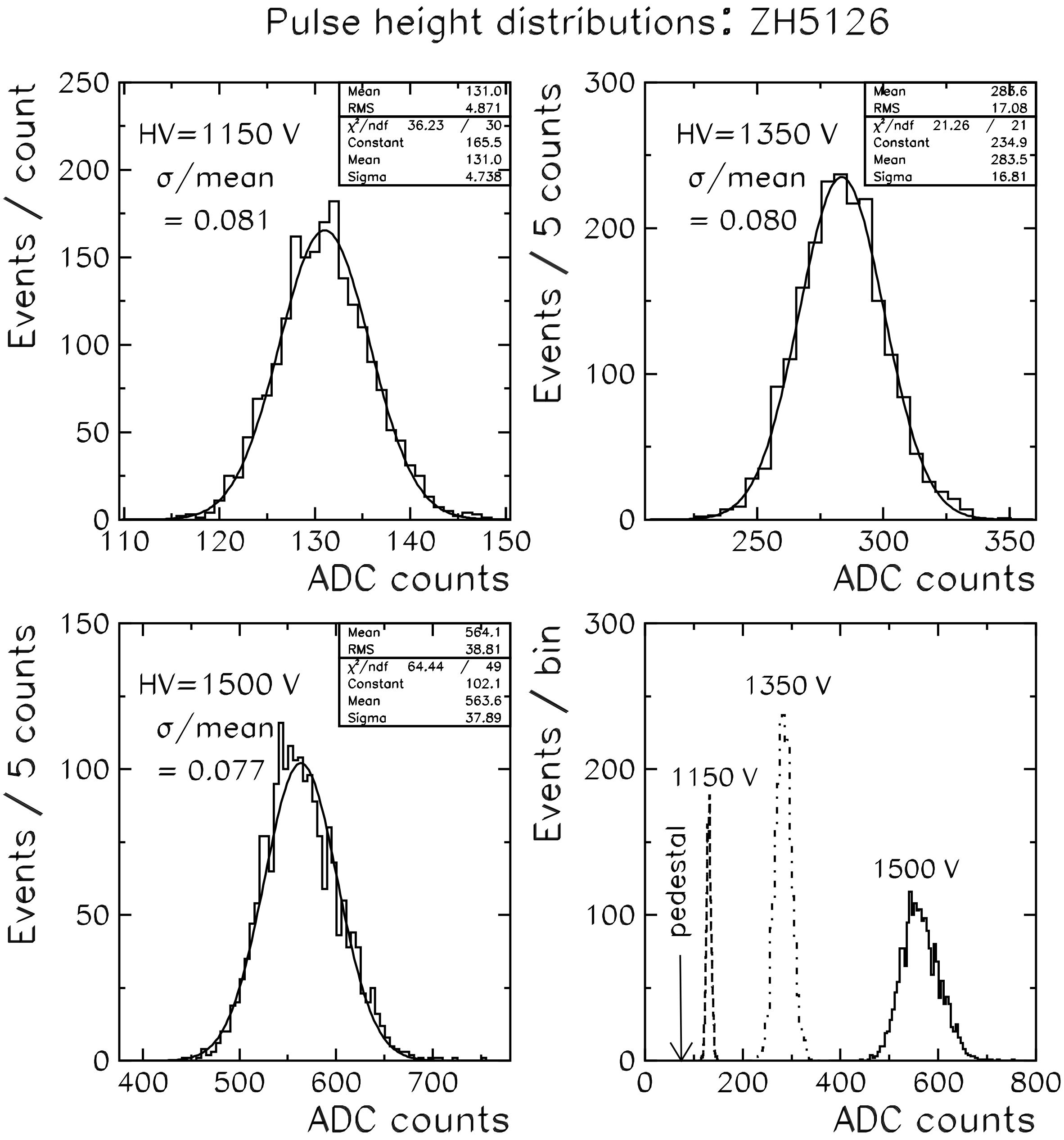

Figure 8: Pulse height distributions for pico-second laser light measured with the tube ZH5126.

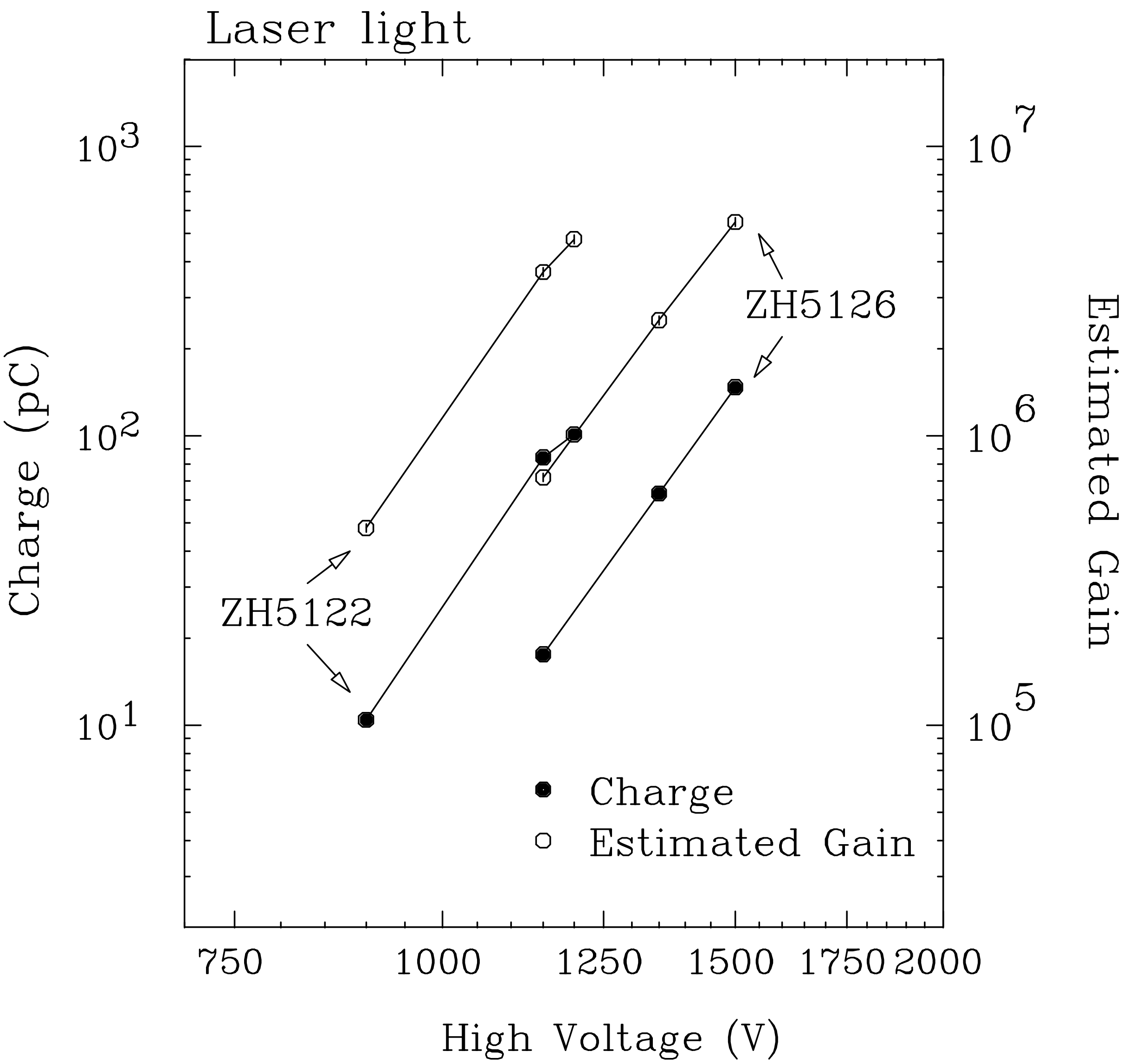

Figure 9: Pedestal-subtracted mean pulse height for laser light as a function of applied high voltage. Also show is the estimated gain.

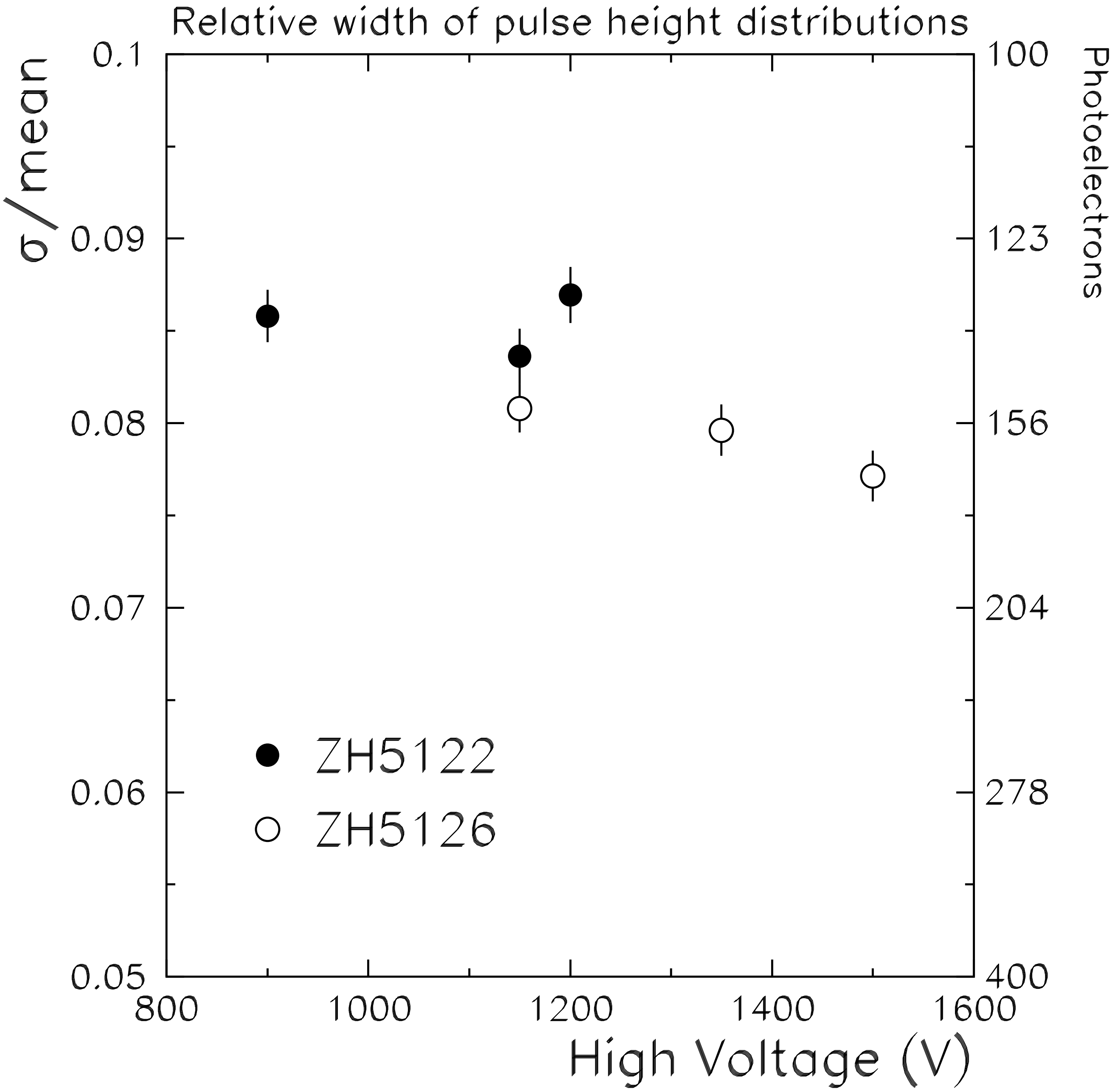

Figure 10: Relative width of pulse height distributions as a function of the applied high voltage.

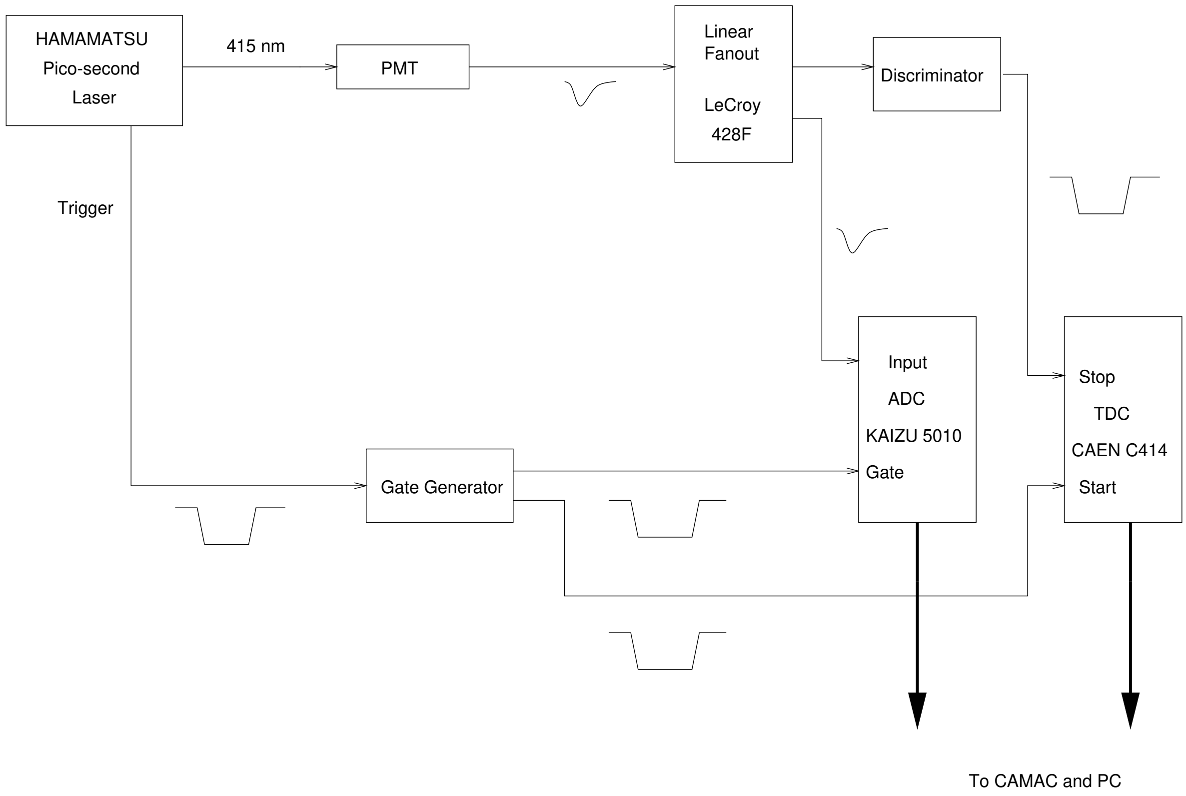

Figure 11: Setup used for the measurement of PMT pulse heights and timing resolutions using a pico-second laser.

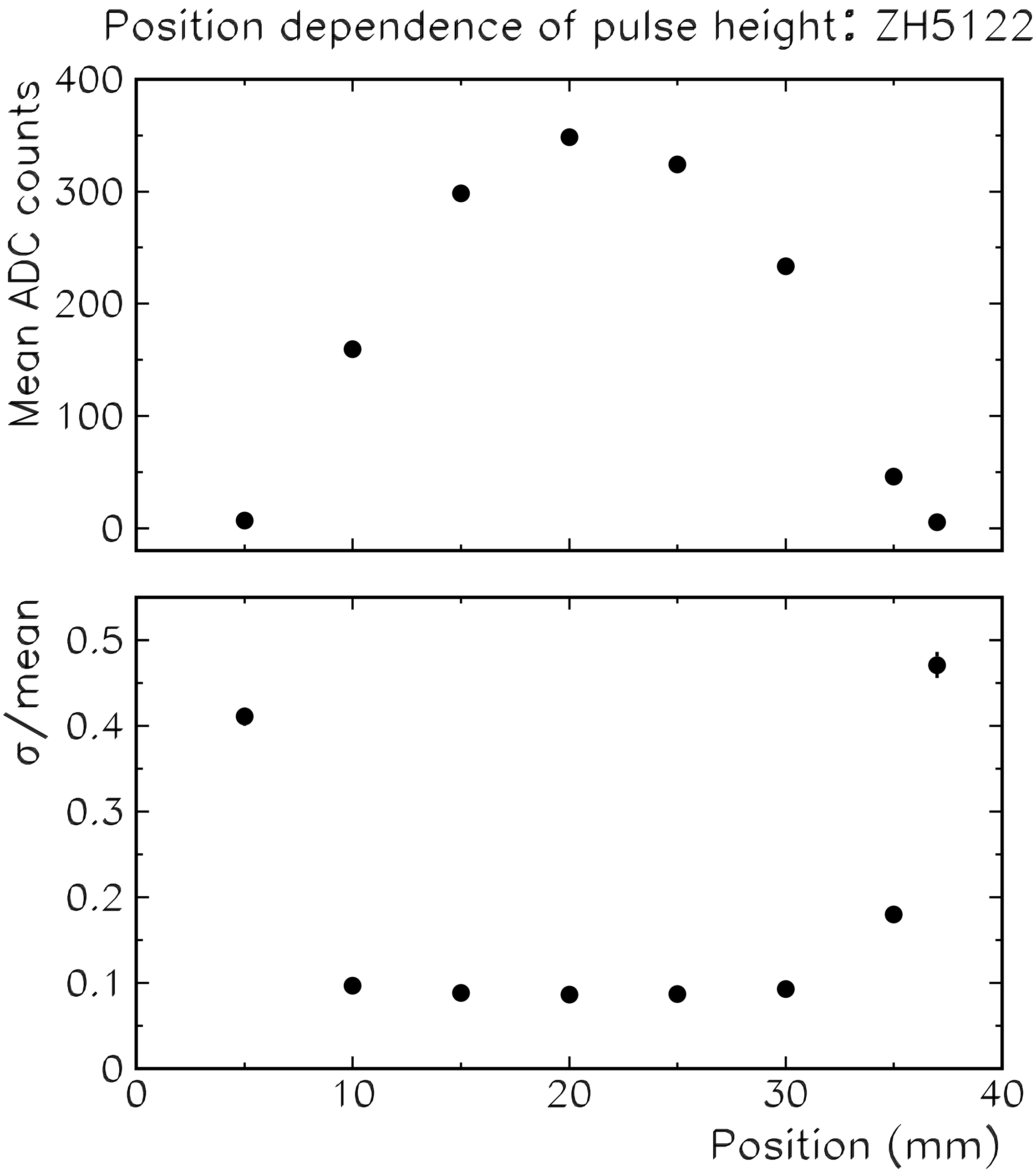

Figure 12: Position dependence of the mean pulse height (top) and the relative width (bottom) measured for the tube ZH5122.

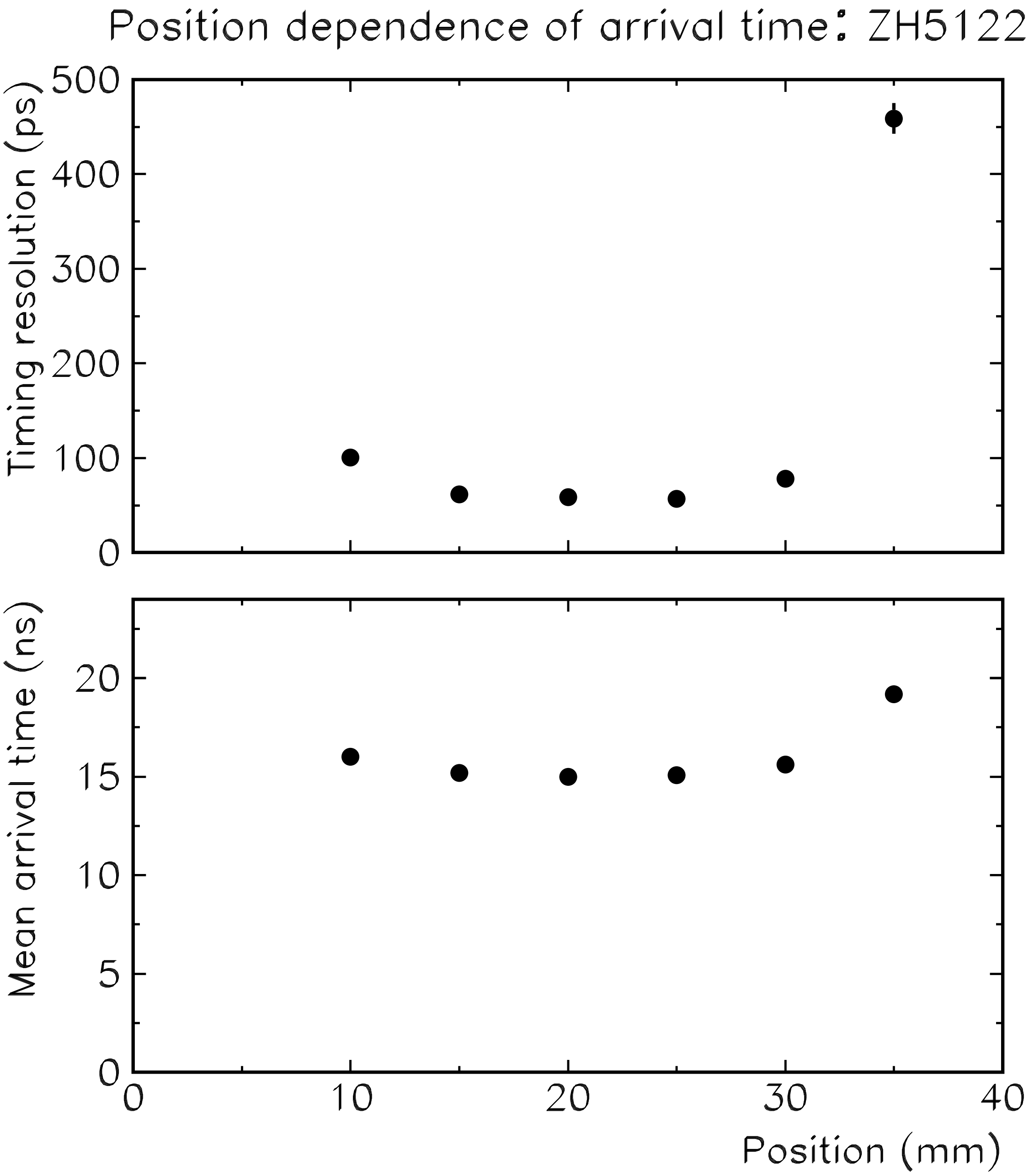

Figure 13: Position dependence of the timing resolution (top) and the mean arrival time (bottom) measured for the tube ZH5122.

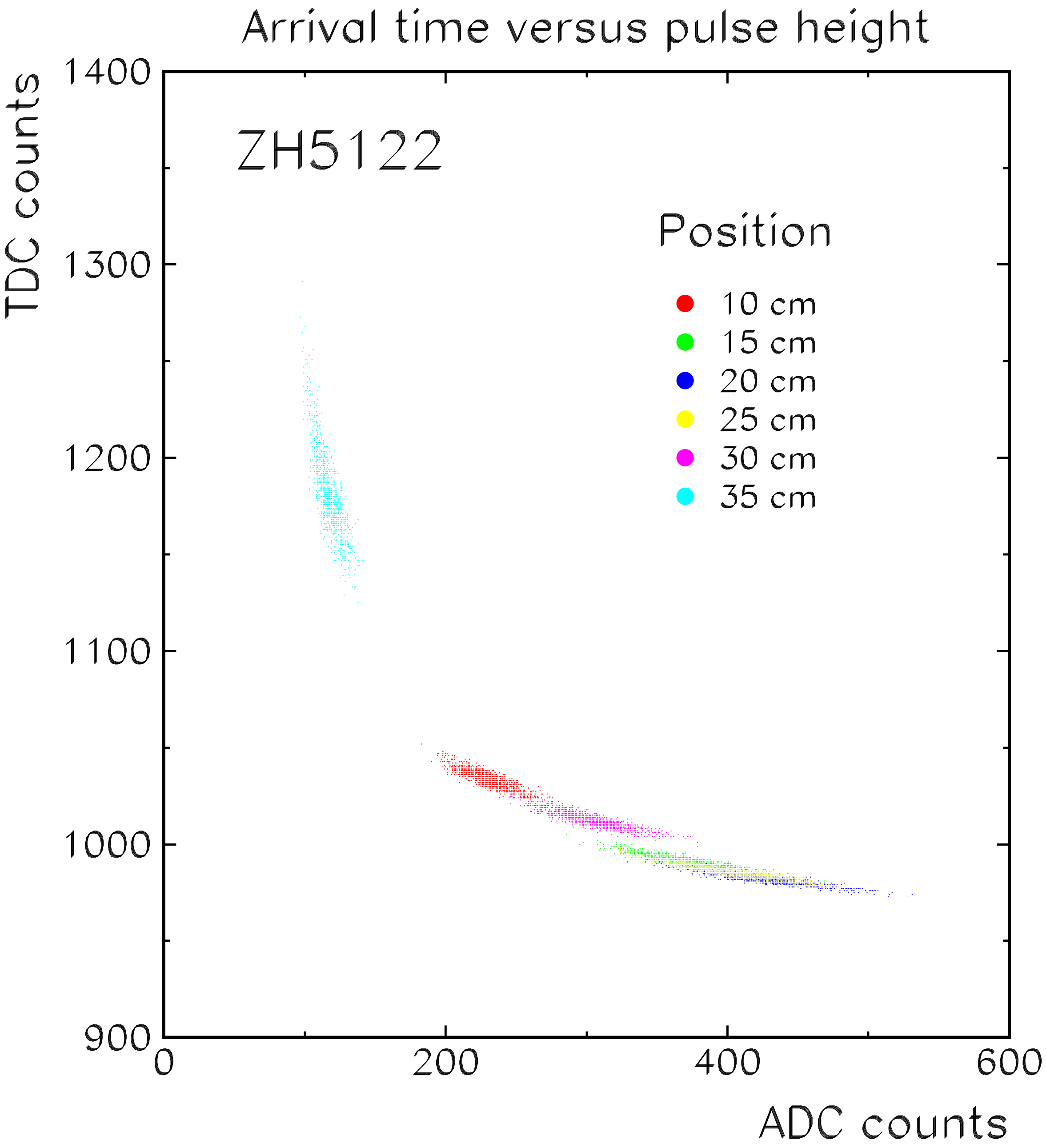

Figure 14: Correlation of the arrival time and the pulse height measured at various positions for the tube ZH5122. Data at different positions are shown in different colors, which can be seen on ghostview.

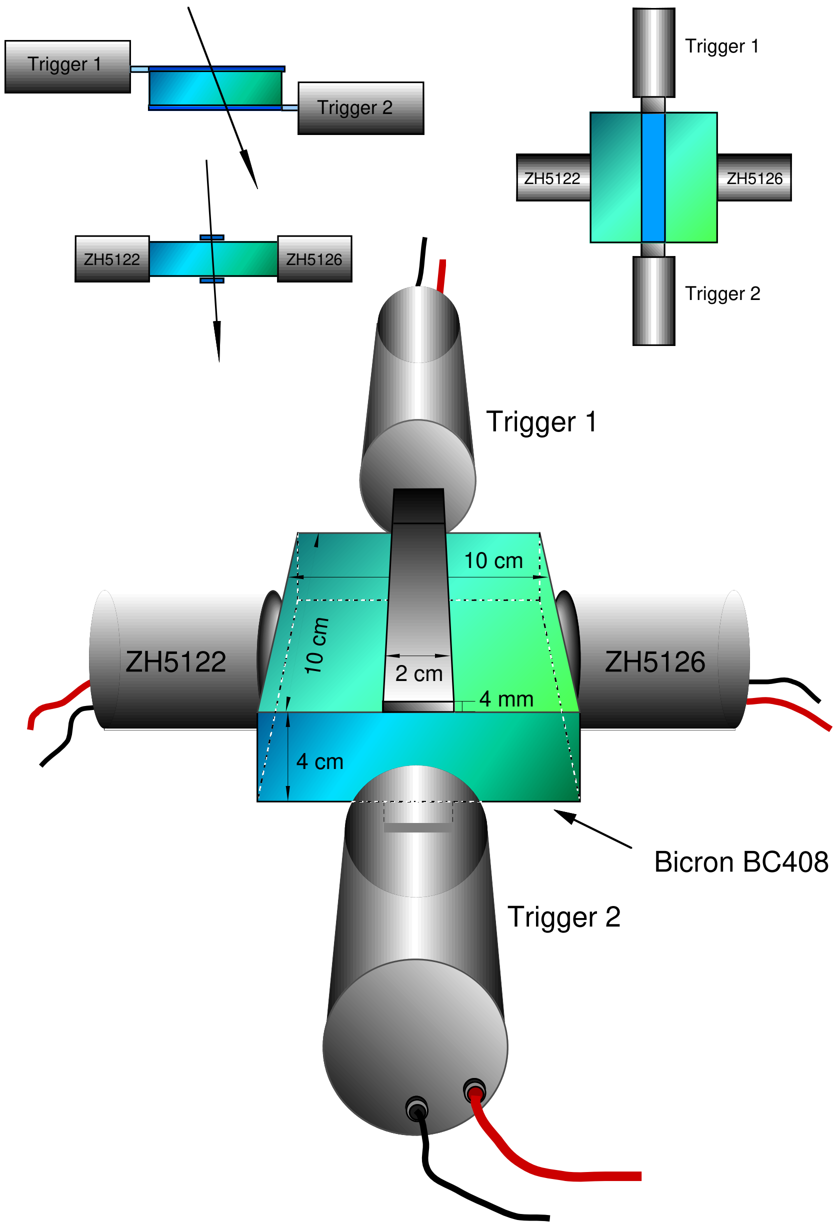

Figure 15: Setup of scintillator, PMTs and trigger counters used for measurements of PMT performance using cosmic rays.

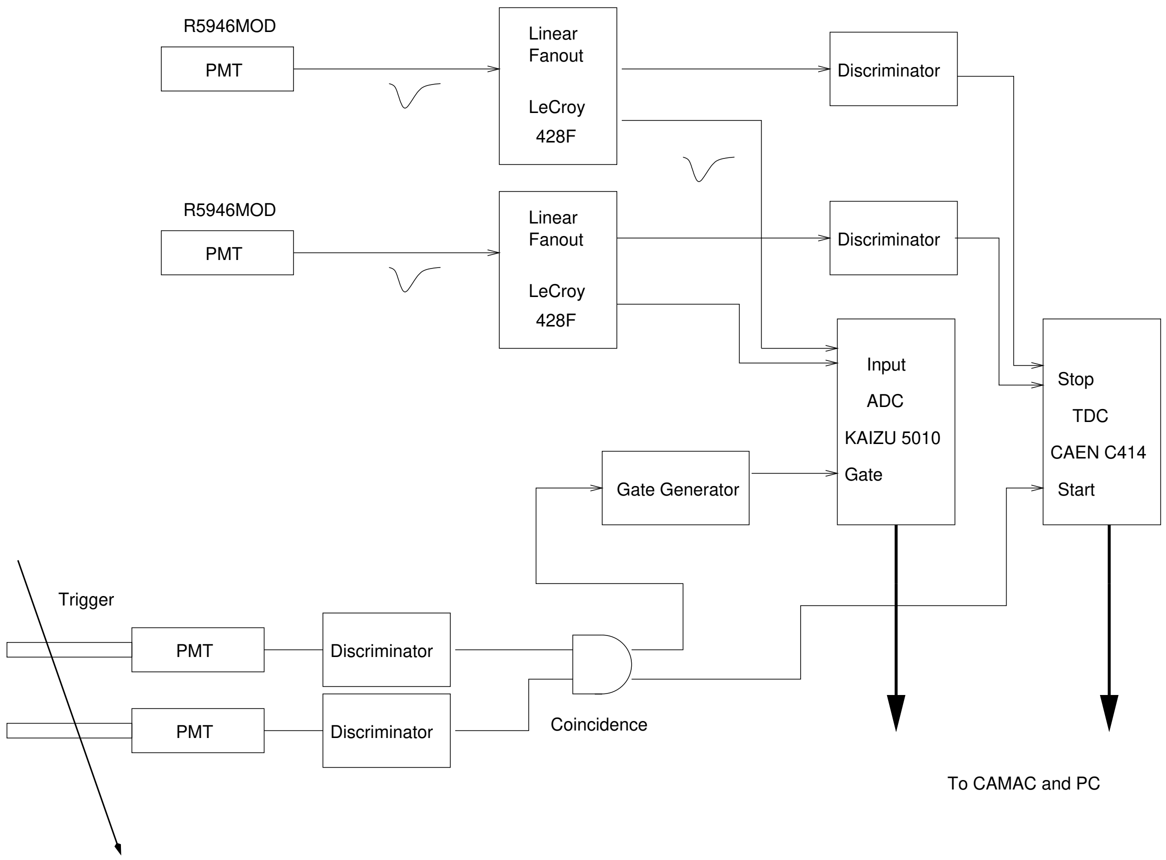

Figure 16: Setup used for measurements of PMT performance using scintillator and cosmic rays.

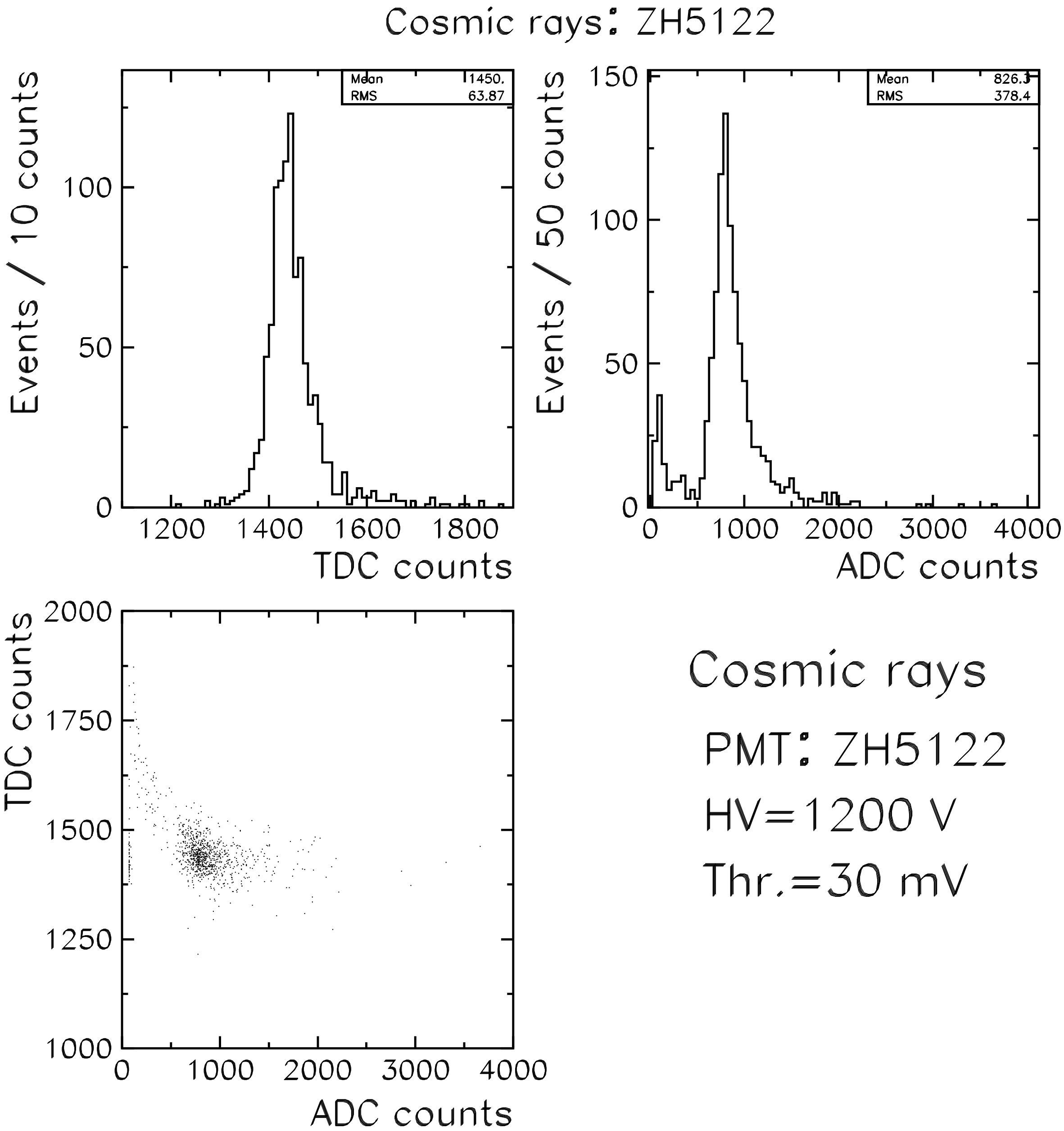

Figure 17: TDC arrival time and ADC pulse height distributions for cosmic rays measured with the tube ZH5122. The high voltage is set to 1200 V, and the discriminator threshold is set to 30 mV.

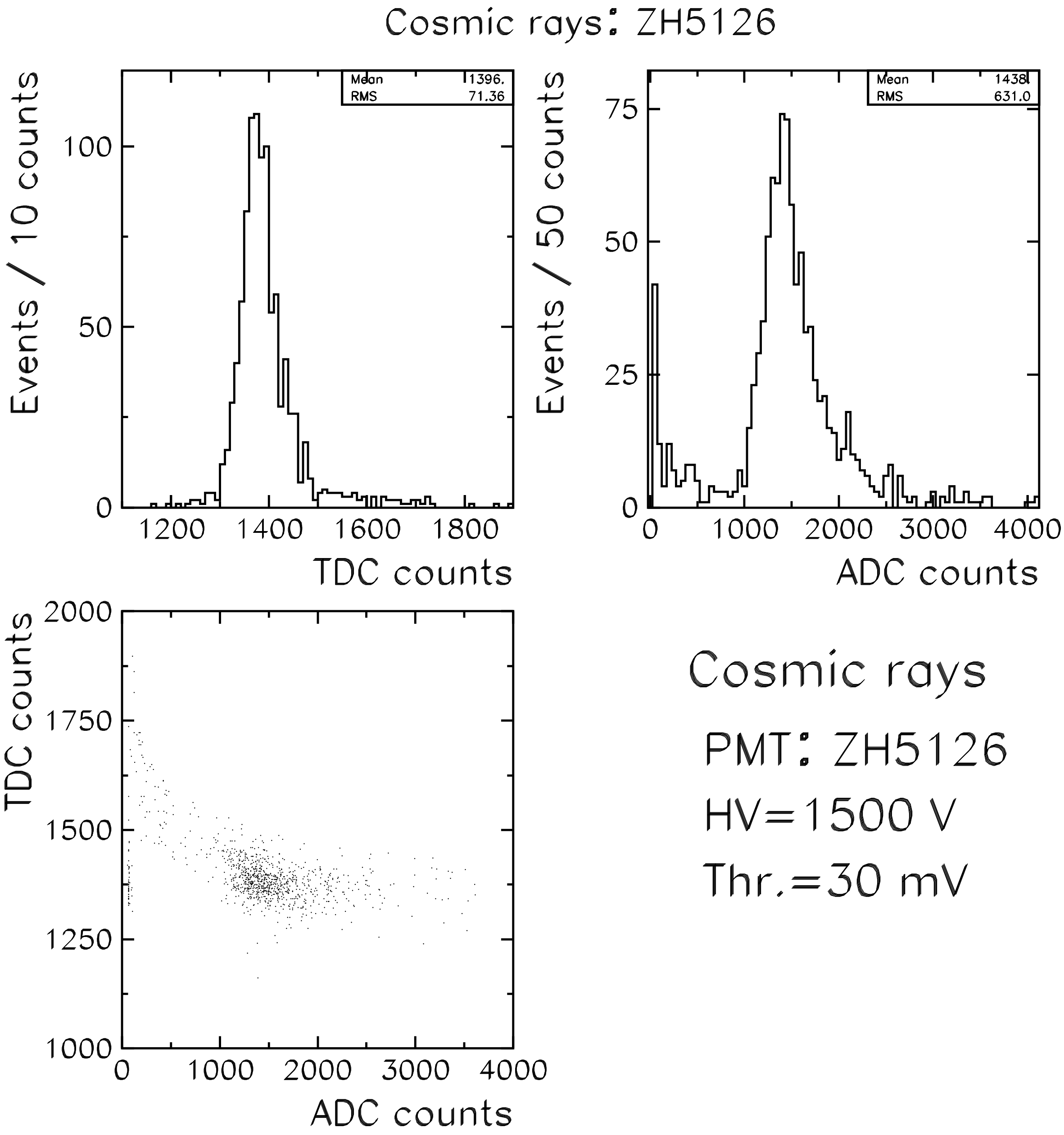

Figure 18: TDC arrival time and ADC pulse height for cosmic rays measured with the tube ZH5126. The high voltage is set to 1500 V, and the discriminator threshold is set to 30 mV.

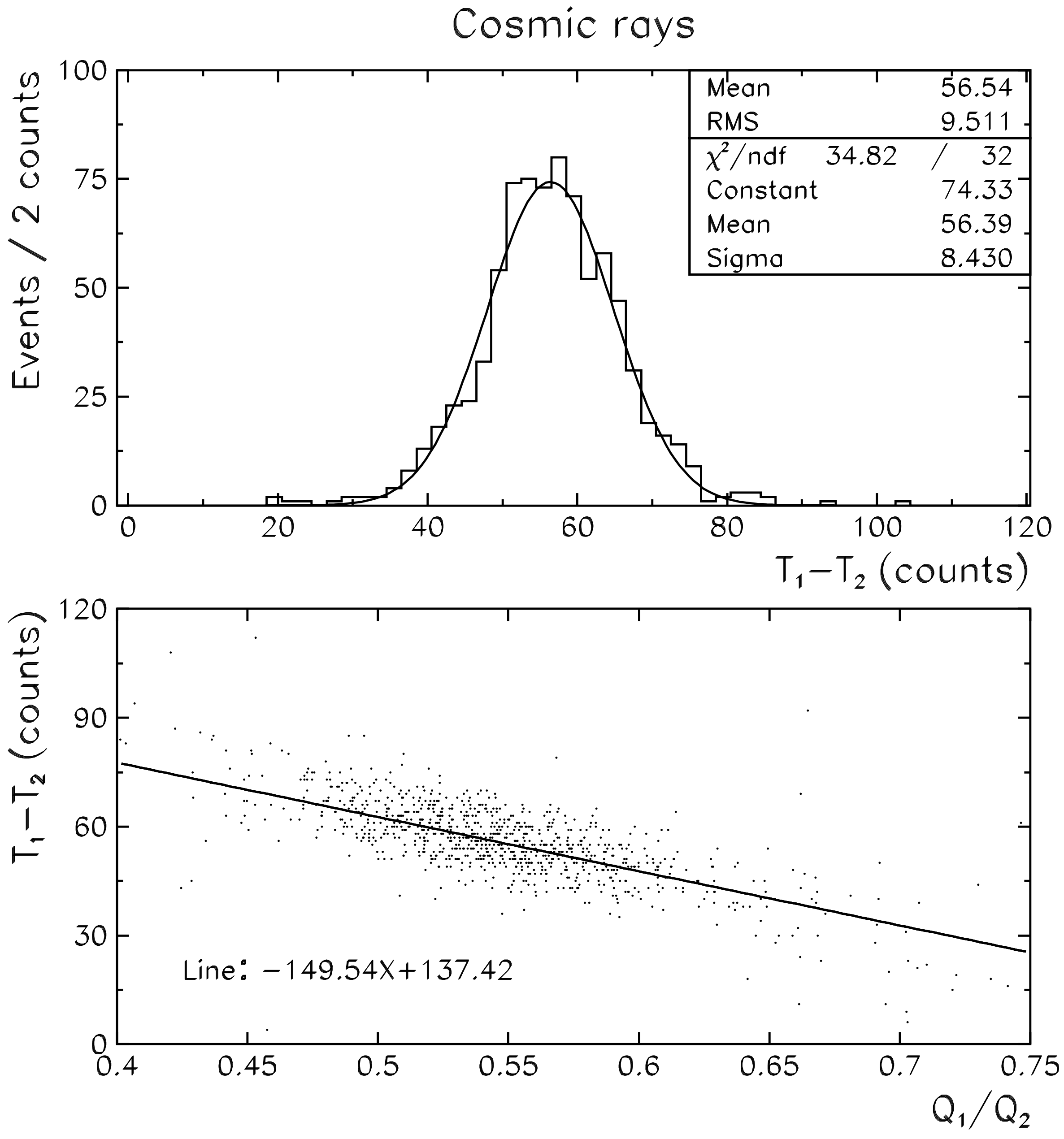

Figure 19: Top: Distribution of the difference in arrival times between tubes ZH5122 and ZH5126 measured for cosmic rays. Bottom: Time difference versus the pulse height ratio.

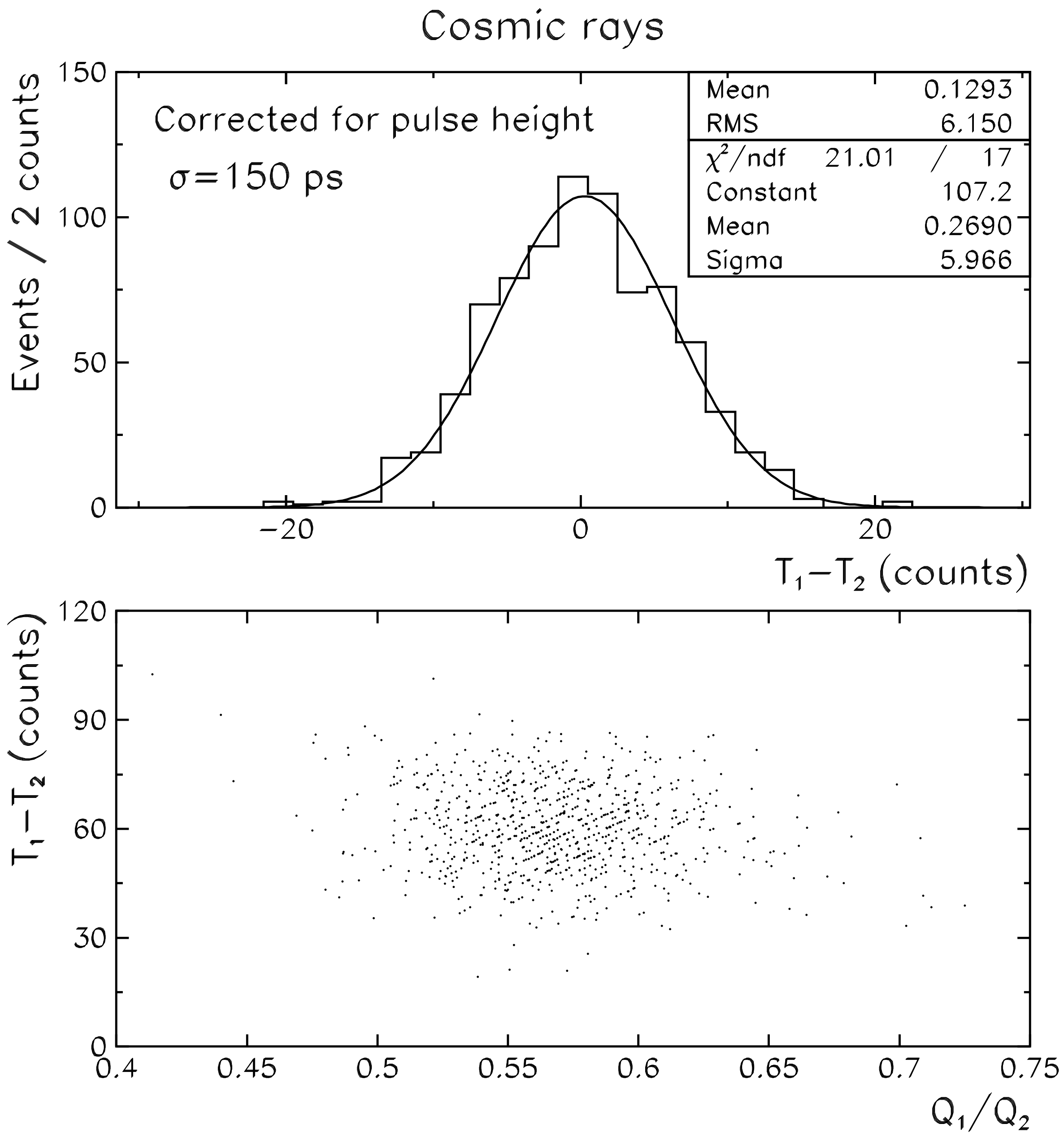

Figure 20: Top: Distribution of the difference in arrival times between tubes ZH5122 and ZH5126 measured for cosmic rays. Corrected for the pulse heights seen in the two tubes. Bottom: Corrected time difference versus the pulse height ratio.